

P. L. Edds-Walton · R. R. Fay

Directional selectivity and frequency tuning of midbrain cells in the oyster toadfish, *Opsanus tau*

Received: 18 September 2002 / Revised: 14 March 2003 / Accepted: 1 May 2003 / Published online: 25 June 2003
© Springer-Verlag 2003

Abstract Single-unit recordings were made from areas in the midbrain (torus semicircularis) of the oyster toadfish. We evaluated frequency tuning and directional responses using whole-body oscillation to simulate auditory stimulation by particle motion along axes in the horizontal and mid-sagittal planes. We also tested for bimodality in responses to auditory and hydrodynamic stimuli. One recording location in each animal was marked by a neurobiotin injection to confirm the recording site. Recordings were made in nucleus centralis, nucleus ventrolateralis, and the deep cell layer. Most units were frequency-selective with best frequencies between 50 and 141 Hz. Suppression of activity was apparent in 10% of the cells. Bimodality was common, including inhibition and suppression of background activity by auditory or hydrodynamic stimulation. The majority of the cells were directionally selective with directional response patterns that were sharpened compared with those of primary saccular afferents. The best directional axes were arrayed widely in spherical space, covering most azimuths and elevations. This representation is adequate for the computation of the motional axis of an auditory stimulus for sound source localization.

Keywords Auditory processing · Directional hearing · Nucleus centralis · Nucleus ventrolateralis · Torus semicircularis

Abbreviations BF: best frequency · DCL: deep cell layer · DON: descending octaval nucleus · DRP: directional response pattern · FFT: fast Fourier transform · LL: lateral lemniscus · NC: nucleus centralis · NVL: nucleus ventrolateralis · PVC: periventricular cells · R: coefficient of synchronization · TS: torus semicircularis · Z: Rayleigh statistic

Introduction

Diversity is great among teleost fishes, both in natural history and in morphology. With respect to hearing range and auditory sensitivity, however, teleosts have been categorized into two groups: the specialists and the nonspecialists. Hearing specialists, such as the goldfish, have accessory peripheral structures that provide sensitivity to the pressure component of underwater sound and extend the hearing range into higher frequencies than those detected by the nonspecialists. The majority of fishes are nonspecialists that probably detect only the particle motion component of underwater sound through a direct, inertial response by components of the ear.

The oyster toadfish (*Opsanus tau*) is a nonspecialist that has a relatively common organization of the auditory system. The ear consists of three endorgans (utricle, lagena, and saccule), each of which has a calcareous otolith that overlies a sensory epithelium of hair cells. The sensory hair cells occur in various directional orientations (Popper and Coombs 1982) on the epithelium. Each hair cell has a best direction of sensitivity to particle motion, and the various orientations on each endorgan determine the directional information that can be obtained from that endorgan.

The saccule of the toadfish is the largest of the otolithic endorgans and is believed to be the primary auditory endorgan in this species (Fay et al. 1994; Fay and Edds-Walton 1997b; Edds-Walton et al. 1999). The paired saccules are oriented primarily in the vertical

P. L. Edds-Walton (✉) · R. R. Fay
Parmly Hearing Institute,
Loyola University Chicago,
Chicago, IL, 60626, USA
E-mail: peddswa@phi.luc.edu

R. R. Fay
Department of Psychology,
Loyola University Chicago,
Chicago, IL, 60626, USA

P. L. Edds-Walton · R. R. Fay
Marine Biological Laboratory, Woods Hole,
MA, 02543, USA

plane at approximately $\pm 30^\circ$ azimuth with 0° as the midline of the fish (illustrated in Edds-Walton et al. 1999). The individual hair cells are oriented in various directions over the surface of the saccular epithelium (Edds-Walton and Popper 1995). Saccular afferents have a robust variety of frequency- and direction-dependent responses that provide information regarding the axis of acoustic particle motion (Fay and Edds-Walton 1997a, 1997b). Encoding and representing the axis of acoustic particle motion in the brain is considered to be the first and most important step in computing the location of sound sources (e.g., Schuijf 1981).

We are interested in the acoustic parameters that are represented at various levels of the auditory system in the toadfish. To investigate this, we have studied auditory processing by primary afferents of the sacculle, and auditory projection sites in the medulla (descending octaval nucleus, DON) and in the torus semicircularis (TS) of the midbrain (Fay and Edds-Walton 1997a, 1997b; Edds-Walton and Fay 1998; Edds-Walton et al. 1999; Fay and Edds-Walton 1999, 2000, 2001). We have found that both frequency and direction are encoded at all three levels. Most primary afferents have a cosinusoidal directional response pattern in the horizontal and mid-sagittal planes, indicating that inputs are equivalent to one hair cell or multiple hair cells having the same orientation. In the DON, however, some single units have compressions of this cosinusoidal directional response pattern (directional sharpening) that we have modeled as arising from simple excitatory and inhibitory interactions among afferent inputs to the DON cells (Fay and Edds-Walton 1999). The goal of this study was to obtain a sample of the response characteristics of cells in the TS, which receives input from the DONs (Edds-Walton 1998) and from a secondary octaval population (reviewed by McCormick 1999).

The location and the connectivity of the teleost TS suggest that it is a homologue of the auditory midbrain of amphibians, reptiles, birds, and mammals (McCormick 1992, Carr 1992), although lateral line processing areas are also present (McCormick 1999, Weeg and Bass 2000). The TS of teleost fishes includes two divisions of primary interest in this study: nucleus centralis (NC) and nucleus ventrolateralis (NVL). Auditory processing is thought to occur exclusively in NC, which is located dorsally in the TS, overlain by a periventricular cell layer (Bass et al. 2000, 2001). The lateral line modality is believed to be processed exclusively in NVL (Bass et al. 2000; Weeg and Bass 2000). This lateral line processing area is ventral to NC in some fish species, but may also lie lateral to NC at the lateral edge of the TS in some species (illustrated in McCormick 1989), including *O. tau* (P.L. Edds-Walton and R.R. Fay, personal observations). Also in the TS, Bass et al. (2000, 2001) identified a group of cells underlying the NVL, which they called the deep cell layer (DCL). This region is of interest because injections into NC produced labeled fibers and terminals in the DCL in the midshipman (Bass et al. 2000).

Our preliminary findings confirmed the presence of frequency and directional selectivity in the TS (Fay and Edds-Walton 2000). Here we report a detailed investigation of cells in the TS to characterize the directional and frequency response properties of cells at various locations. We used a three-dimensional micromanipulator to map relative locations in the TS and small neurobiotin injections to label a single recording site in each fish. The label site functioned as a method of confirming our recording location and evaluating the relative location of other recording sites in the same fish. In addition, we have made qualitative observations of what we believe is bimodality among TS cells (Fay and Edds-Walton 2001). Specifically, some TS cells respond to both whole-body motion designed to activate the auditory system and to hydrodynamic stimuli that most likely activate the lateral line system.

Materials and methods

Experimental procedures

Male and female toadfish were acquired from the Marine Resources Center at the Marine Biological Laboratory, Woods Hole, MA. All were adults captured from local waters during the months of June and July (standard length 16.8 ± 1.65 cm; mean \pm s.d.). This encompasses the peak of the breeding season for this species and most females had eggs. The toadfish were maintained in a flow-through saltwater tank at $12\text{--}15^\circ\text{C}$ and were fed squid chunks, clams, or goldfish. The maintenance and experimental procedures were approved by the Animal Care and Use Committee of Loyola University Chicago and the Marine Biological Laboratory.

Prior to each experiment, fish were anesthetized in seawater with 3-aminobenzoic acid methane-sulfonate salt (1:1,000; Sigma) and immobilized with an injection of pancuronium bromide (0.05 mg kg^{-1}). Lidocaine was applied to the skin of the head as a topical analgesic prior to surgery and reapplied to the edges of the surgical opening in the skin every 3 h. Care was taken to prevent the lidocaine from entering the skull. After reflecting the skin and muscle, the skull was entered on the left side through the parietal bone. The opening was enlarged across the midline suture to reveal the left optic tectum in its entirety, as well as part of the right optic tectum to permit measurements of location using the midline of the midbrain as a landmark (Fig. 1A). The meninges of the brain were removed carefully without damage to the blood flow around the brain. The fluid level in the cranial cavity was maintained by the addition of an inert fluorocarbon liquid (FC-77, 3M).

After surgery, the fish was transferred to an aluminum cylindrical dish (diameter 23 cm, height 8 cm, wall thickness 0.5 cm) containing seawater. A rigid holder was used to secure the head of the fish to the cylindrical dish. The depth of the seawater was kept at a level just below the surgical opening in the skull. Since water flow could interfere with our experimental stimuli, water changes were done every 2 h to maintain sufficient oxygen levels, remove any wastes produced by the fish, and maintain the temperature between 18 and 20°C . A large syringe was used to exchange 500 ml of seawater (approximately half the volume of the dish).

The cylindrical dish was suspended by two pneumatic vibration-isolation systems (Micro-G). Paired moving-coil shakers attached to the sides, front, and rear of the dish produced sinusoidal motion along linear pathways in the horizontal plane. A single vertical shaker produced sinusoidal motion of the dish on the vertical axis. Translational motion was generated in three-dimensional space by specifying amplitudes and phases of sinusoids operating the three shaker channels (side-side, front-back, and vertical) to the dish. Signals were digitally synthesized, 500-ms

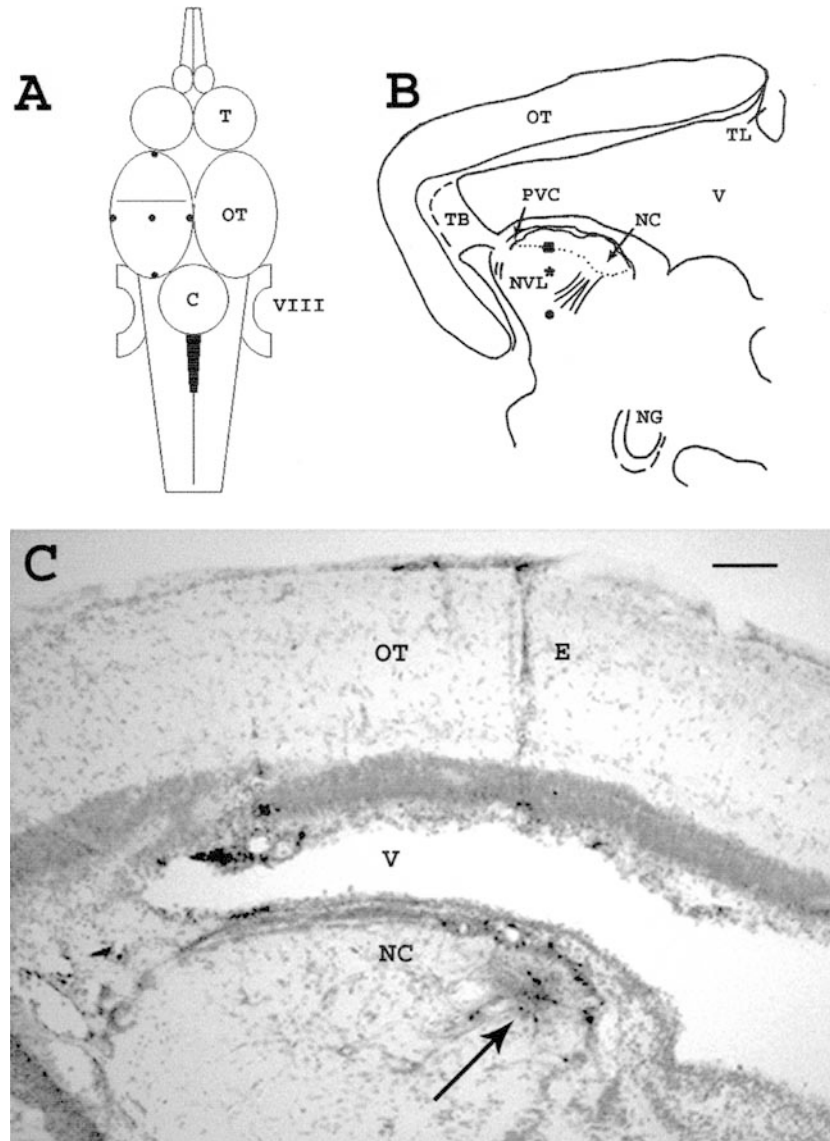


Fig. 1A–C Toadfish brain. **A** Representation of the dorsal view of a toadfish brain. All recordings were conducted through the intact, left optic tectum (*OT*). Standardized measurements were taken of the tectal surface along with depth of the recording site. The line through the tectum illustrates the approximate level at which **1B** was drawn. *C* cerebellum, *T* telencephalon, *VIII* acoustic cranial nerve. **B** Diagram of transverse section through the rostral midbrain. Three recording sites are shown. The *asterisk* represents the injection site, which was the location of a bimodal cell in nucleus ventrolateralis (*NVL*). The locations of the other two sites were based on the numbers recorded from the 3-D micromanipulator during the recording of an auditory-only cell (*square*, at ventral border of nucleus centralis, *NC*), and a cell suppressed by auditory stimulation (*circle*, in the deep cell layer, *DCL*). A bundle of fibers present in this area (called the diagonal band by Bass et al. 2000) is also illustrated as parallel lines. *NG* nucleus glomerulosus, *OT* optic tectum, *PVC* periventricular cells, *TB* tecto-bulbar tract, *TL* torus longitudinalis, *V* ventricle. **C** Photomicrograph of a section through the midbrain at a recording site injected with neurobiotin (*arrow*). Note that this is not the same experimental brain shown in **B**. *E* electrode track through the tectum, *NC* nucleus centralis, *OT* optic tectum, *V* ventricle. scale bar = 100 μm

sinusoids (20 ms rise and fall times), read out of TDT (Tucker Davis Technologies, Gainesville, Fla., USA) 16-bit digital-to-analog converters (10 kHz sample rate), low-pass filtered (2 kHz), attenuated (TDT PA4 programmable attenuators) and amplified (model 5507, Techtron, Elkhart, Ind., USA). The amplified signal was attenuated (32 dB) by fixed-power resistors to reduce amplifier noise and improve signal-to-noise ratio at the shakers.

Dish movement was calibrated prior to every experiment, after the fish was secured, by monitoring the activity of three, orthogonally oriented accelerometers (PCB model 002A10, Flexcel, Piezotronics, Depew, N.Y., USA; sensitivity = 1 v/g of acceleration) permanently mounted to the outer surface of the dish with cyanoacrylic glue. The calibration series consisted of the standard stimulus generation programs used during experimentation. The specially designed calibration program generated a graphical representation of dish movement by plotting the accelerometer outputs and calculating displacement levels in decibels with respect to 1 nm, root-mean-square (rms).

Physiological data were collected as follows. The tip of a pulled glass electrode was broken to a diameter of 2–5 μm . The electrodes had resistances of 5–20 $\text{M}\Omega$ when filled with 4% neurobiotin (Molecular Probes) in 3 mol l^{-1} NaCl. The electrode was lowered to the surface of the left optic tectum and the location was

recorded. Then the electrode was lowered through the optic tectum and the ventricle, and into the TS. The stimulus program was initiated in the search mode (circular or omnidirectional stimulation at 100 Hz), and the electrode was lowered slowly until neural activity was heard on the audio monitor. After a TS unit was contacted extracellularly, spontaneous or background activity was estimated by acquiring spike counts over eight, 500-ms periods without deliberate stimulation.

The 18 experimental stimuli consisted of eight repetitions of the 500-ms sinusoidal stimulus in specified directions, frequencies, and levels. Stimulus presentation was completely automated. Eleven 100-Hz directional stimuli were first presented in a predetermined order that consisted of six axes in 30° increments in the horizontal plane, nominally from 90° (side-to-side) to 240°, and five additional axes at 30° increments in the mid-sagittal plane from 30° to 150°. Front to back (0° elevation) data were taken from the 0° stimulus presentation in the horizontal plane. These stimuli were followed by a series of seven stimuli (at 330° azimuth in the horizontal plane to maximize stimulation of the left saccule) at frequencies of 50, 60, 84, 141, 185, 244, and 303 Hz at equal displacement levels, generally in the range of 0–20 dB re: 1 nm (rms). Data for 100 Hz were taken from the 330° stimulus presentation in the horizontal plane. Typically, this automatic stimulus presentation was repeated at several levels in 5-dB increments within the neuron's dynamic range. In selected cases, response-versus-level functions were determined for stimuli at three orthogonal stimulus axes: up-down (90° elevation), side-side (90° azimuth, 0° elevation), and front-back (0° azimuth and 0° elevation).

Spikes were discriminated using a single voltage criterion, and spike times were recorded with 0.1-ms resolution. Response magnitude was defined in terms of spike rate (spikes s⁻¹). Spike rate data were used in estimates of background activity, in defining iso-level, frequency response areas (spike rate as a function of frequency), and iso-level, directional response profiles (DRP).

Hydrodynamic stimulation was added to the stimulus set after locating numerous cells in the TS with background activity that did not respond to the auditory stimulus. A flashlight was used for on/off light stimulation, but no response was obtained. We used a vibrating sphere underwater (driven by a minishaker) along the length of the fish, from head to tail to head, but did not obtain consistent responses. Finally, we tried puffs of air on the surface of the water to produce a more extensive hydrodynamic stimulus from head to tail to head repeatedly, along the length of the fish, ipsilateral (left) and contralateral (right). This stimulus produced consistent increases or decreases in background spike activity for the cells that did not respond to auditory stimuli. The inclusion of this stimulus for all cells revealed cells that responded to both the hydrodynamic stimulus and auditory stimuli. We have classified those as bimodal cells.

We tested the response of primary lateral line afferents in the oyster toadfish to the air puff stimulus in a preparation by L. Palmer. The body of the fish was immersed in water to a depth just below the surgical opening in the top of the skull. Palmer placed an electrode in the anterior lateral line nerve to record primary afferent activity extracellularly (Palmer and Mensinger 2003). A predictable, transient increase in spike activity occurred when individual squirts of water (using a bulb pipet) were directed around the head and when our puffs of air directed at the water surface produced water movement around the fish. Tricus and Highstein (1990) also recorded from the anterior lateral line nerve while using "fine jets of water" around the head and obtained correlated afferent responses. Based on those observations, we believe the water movement induced by the air puffs at the surface activated lateral line receptors, though we did not determine which component was stimulated (canal or superficial neuromasts).

We also conducted two tests to be certain that the ear was not being stimulated by the air puffs. First, the air puffs were produced over the normal volume of water in the experimental dish, without the fish present, to determine whether the air puffs could move the dish. The calibration program was used to monitor dish movement with the accelerometers (which are sensitive to nanometer movements in all three planes). Given that the fish is attached to the dish,

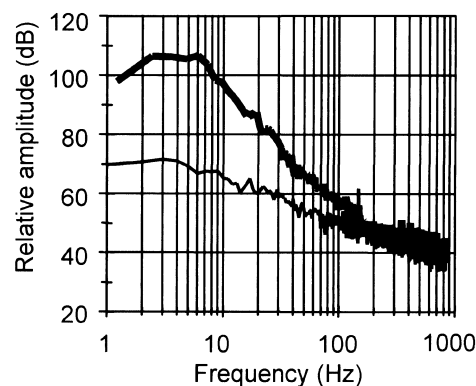


Fig. 2 Power spectrum of the hydrodynamic stimulus. The spectrum of ten air puffs on the water surface (*thick line*) was characterized using a hot-film anemometer system and averaged (see text and Coombs et al. 1989). The anemometer probe was positioned below the surface in line with the direction of the hydrodynamic stimulus. Note that the majority of the acoustic energy is below 10 Hz, with a low-pass roll-off above 10 Hz of 43 dB/decade. At 70 Hz, the level of the stimulus is equivalent to background noise (*thin line*; in quiet)

the dish would have to move for the air puffs to stimulate the ear of the fish via particle motion. We conducted three tests with puffs of air on each side of the dish, and three tests of dish movement with no stimulus, equivalent to 'background' or random movements of the dish, which is suspended on an air table. The average movement of the dish in both cases did not differ.

Secondly, the power spectrum of the hydrodynamic stimulus was characterized using a hot-film anemometer system (TSI, Shoreview, Minn., USA) as described and evaluated by Coombs et al. (1989). Although an anemometer nominally measures flow velocity, this system was shown to be displacement-sensitive at frequencies up to 200 Hz (Coombs et al. 1989). The anemometer probe was positioned in the center of the shaker dish, 1 cm below the water surface, with its most sensitive plane oriented vertically and in line with the direction of the air puff. The air puffs were directed at the water surface above the probe and repeated ten times while the voltage signal from the system was digitized for 4,096 points at 5 kHz. The fast Fourier transforms (FFTs) of these sample waveforms were averaged and expressed in decibels (with an arbitrary reference) and compared to the same measurements made in nominal quiet. The data show that most of the air puff energy was in the frequency range between 1 and 10 Hz, with a low-pass roll-off above 10 Hz of 43 dB/decade (Fig. 2). We do not know the frequency response of the receptor organ mediating responses to this stimulus, but it seems likely that the superior effectiveness of the hydrodynamic stimulus for evoking responses in the midbrain cells investigated here arose from its maximal energy and best signal-to-noise ratio in this very low-frequency range.

Further evidence that the ear was not stimulated by the hydrodynamic stimulus comes from our physiological data that show our most sensitive auditory cells did not respond to the hydrodynamic stimulus (Fig. 3C). Based on our evaluations of stimulus parameters and our physiological data, we are convinced that the hydrodynamic stimulus activated a separate sensory modality, not the auditory hair cells of the ear. Given that the anterior lateral line nerve projects to nucleus medialis (Highstein et al. 1992), and that nucleus medialis sends projections to the TS in toadfish (Edds-Walton 1998; Weeg and Bass 2000) and other teleosts (reviewed in McCormick 1989, 1999), the lateral line is very likely to be the second sensory modality.

We routinely used the hydrodynamic stimulus to test all cells in the TS for bimodal activity. The stimulus was applied for the same duration as the particle motion stimuli (8×500 ms). In some cases, the hydrodynamic stimulation was applied during simultaneous

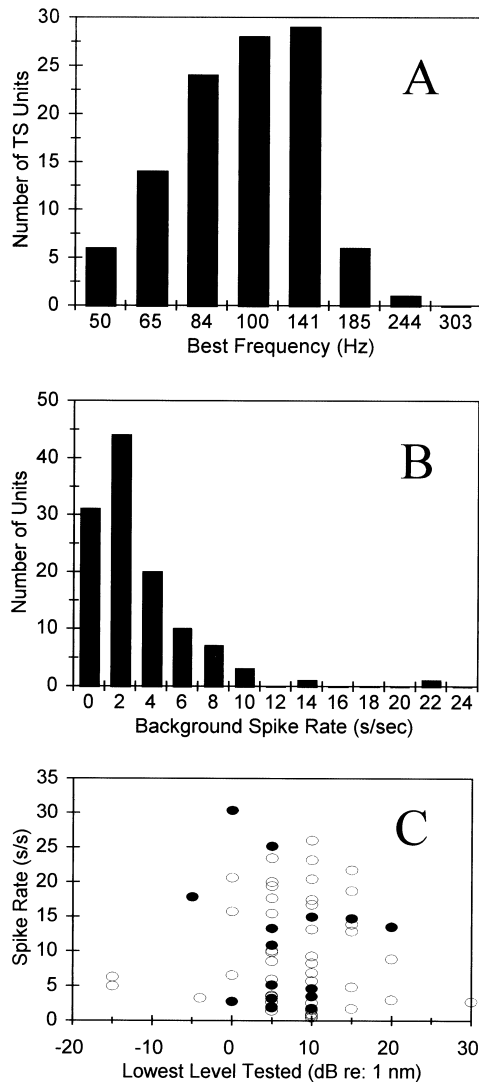


Fig. 3A–C Response characteristics of cells in the torus semicircularis (TS) of the toadfish (*Opsanus tau*). **A** Distribution of best frequency (BF) for recording sites in both NC and NVL. **B** Distribution of average background activity recorded in the absence of directional particle motion stimuli and the hydrodynamic stimulus. Recording sites were in NC and NVL. **C** Average spike rates (from eight repetitions) in response to directional particle motion stimuli, plotted at the lowest level tested (independent of direction). The filled ovals represent bimodal cells that responded to the particle motion stimuli and the hydrodynamic stimulus. The open ovals represent auditory-only cells. Note that the most sensitive cells were not bimodal, indicating that the hydrodynamic stimulus probably did not stimulate the ear

shaker stimulation to investigate their interactions. As with the particle motion stimuli, response magnitude was defined in terms of spike rate (spikes s^{-1}).

Following physiological characterization of a cell, the location of the electrode was recorded for all three axes of the 3-D micro-manipulator (scale: 1 unit = 10 μ m) and the surface of the tectum was recorded at that location to calculate depth of the recording site. One site was labeled in each fish by iontophoresis of neurobiotin (see below). In most cases, the neurobiotin electrode was replaced with one containing only 3 M NaCl for subsequent recording of additional TS units at other sites. However, no recordings were done in the immediate area of a neurobiotin injection to prevent any distortion of the label distribution around

that recording site. At the end of the experiment, the 3-D micro-manipulator was used to obtain coordinates for the edges and approximate center of the tectal surface to assist in mapping the recording sites. These points are indicated on the general outline of the toadfish brain in Fig. 1A. The slight curvature of the tectum was not taken into account. The length and width of the tectum were calculated to compare the relative locations of recording sites among fishes. The location of a recording site was calculated as the percentage distance from the lateral edge (x) and percent distance from the rostral edge (y) of the tectum using the in vivo measurements taken during and following data collection. Depth (z) was calculated as the in vivo distance below the tectal surface.

Three recording sites are shown in a typical drawing of a cross-section in Fig. 1B: one at the NC/NVL border, one in NVL (asterisk) and one in the DCL. The middle site was the final recording site and the one injected in that fish. The location of the cross-section is approximately at the line shown in Fig. 1A. A photomicrograph is provided to illustrate the restricted size of a neurobiotin injection at a recording site in medial NC (Fig. 1C).

Neurobiotin injections and histology

Neurobiotin injections were done at recording sites when that particular site had well-defined spikes and yielded a complete data set. Injections were generally 2,000 nA (electrode positive), for pulsed current with a 50% duty cycle for 10–25 min. The shortest injection time was used to label the recording site with little or no neuronal transport intended (e.g., Fig. 1C), and the fish was sacrificed 10 min after the injection was completed. Longer injection times were used to label the site as well as the processes of cells projecting to that site. The fish with long injection times were incubated for 4–12 h in aerated, chilled seawater taken from their home tank. At the end of the incubation time, the fish was anesthetized deeply, measured and sexed, then perfused with saline followed by buffered 4% paraformaldehyde. The skull was immersed in the fixative overnight. Following dissection, the brain was rinsed in buffer, then placed in 40% buffered sucrose for cryoprotection. Frozen sections (50 μ m) were obtained with a cryostat (Microm HM505N) and were placed in chilled phosphate buffer with 0.9% NaCl (0.1 mol l^{-1} PBS). A standard ABC-DAB reaction (Molecular Probes, Elite) with metal intensification (modified from Hancock 1982) was used on floating sections to visualize the neurobiotin. Sections were placed on slides, lightly counterstained with cresyl violet, and coverslipped for detailed examination. Each brain was examined for the location of the injection site, cells labeled at the injection site, and retrograde label in nuclei with projections to the injection site. Drawings were done at 40 \times , 100 \times , and 400 \times using an Olympus BX50 with a drawing tube, and digital photographs were taken with the Olympus DP12 camera system.

Results

The majority of cells in the TS of the toadfish had little or no background activity (Fig. 3B). The frequency distribution of background spike rates has a prominent mode (29%) at 0–0.5 spikes s^{-1} . The maximum rate was 24 spikes s^{-1} . The range of activity in response to the frequency, directional, and hydrodynamic stimuli are described in detail below.

Frequency response

Best frequency (BF) was defined as the frequency evoking the highest spike rate. When this value varied

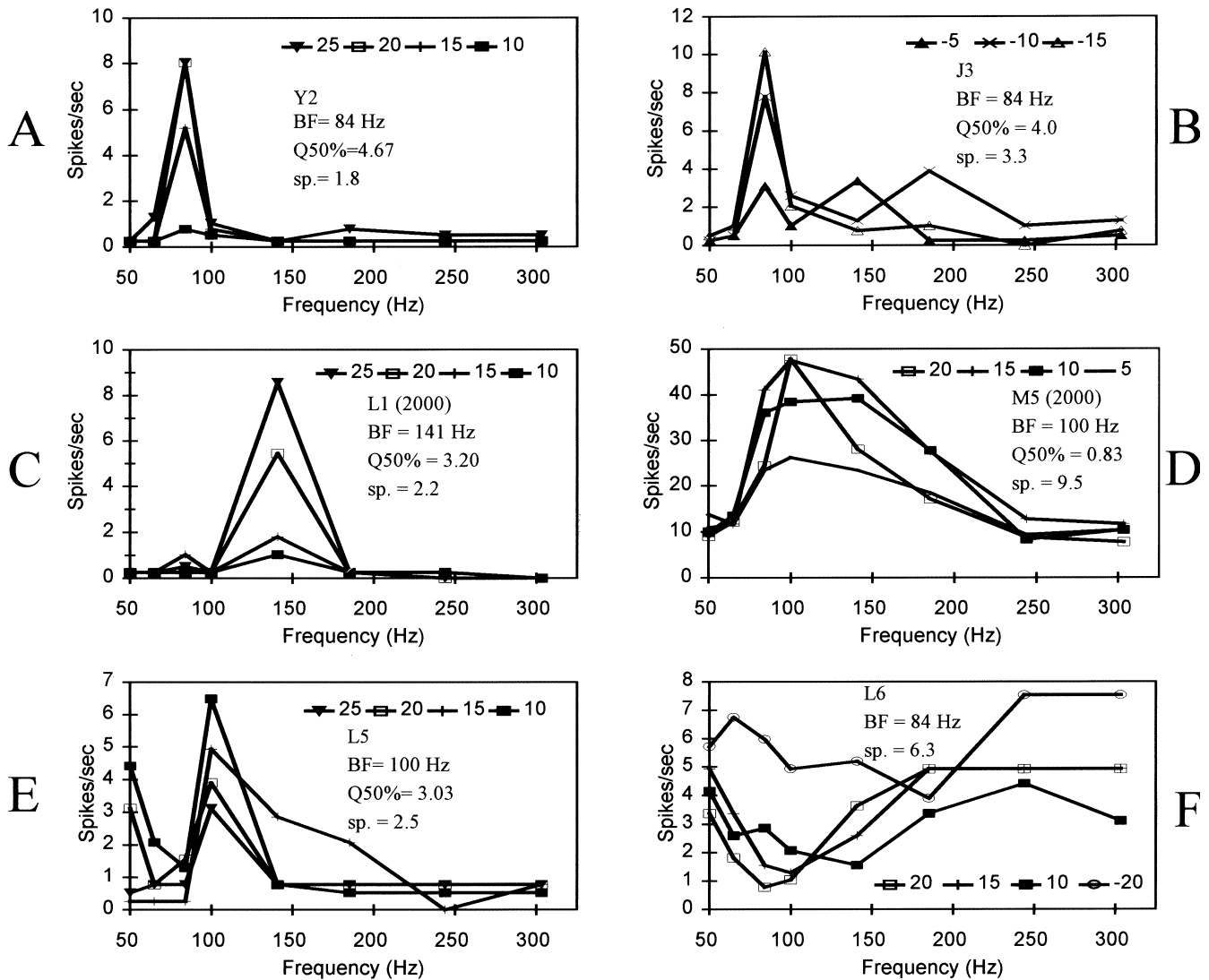


Fig. 4A–F Representative frequency responses for cells in the torus semicircularis of the toadfish. Note that the BF was defined as the frequency evoking the greatest increase in spike rate at the lowest level stimulus presented. The letter and number refer to the fish and cell respectively, and (2000) indicates data obtained that year. Three to four stimulus levels are represented with different symbols on each graph. Frequency selectivity was defined as $BF/BW_{50\%}$, or $Q_{50\%}$. **A** Unit Y2 had sharp tuning at 84 Hz and a small dynamic range (between 10 and 20 dB). **B** Unit J3 had very sharp tuning (BF = 84 Hz). **C** Unit L1 demonstrates a level-independent, high BF of 141 Hz. **D** Unit M5 had a relatively wide frequency response bandwidth, and a contraction of bandwidth at the highest signal level (open squares, 20 dB). **E** Unit L5 exhibited two peaks in the frequency response function (at 50 and 100 Hz) and decreased activity at 100 Hz with increasing stimulus level. **F** L6 is a bimodal cell whose background activity was suppressed by increasing levels of auditory stimulation. sp spontaneous activity (spikes s^{-1})

with signal level, the BF was defined as that for the lowest signal levels presented. BF was determined for 108 units in the TS (Fig. 3A). The range of BFs includes each of the stimulus frequencies presented, except for 303 Hz. The cells classified as having a BF of 50 Hz may have a BF at a lower frequency since frequencies lower

than 50 Hz were not presented. The majority of cells ($85/108 = 79\%$) had a BF between 84 and 141 Hz.

Units of the TS vary widely in their frequency selectivity or tuning. Bandwidth (BW) was defined as the frequency range at a spike rate 50% of the maximum at BF, and selectivity was defined as $BF/BW_{50\%}$, or $Q_{50\%}$. The average $Q_{50\%}$ value for 93 TS units evaluated was 2.43 (s.d. = 0.86), with a range of 0.76–4.42. These figures do not include units with BF = 50 Hz since a bandwidth could not be defined for these units.

The frequency responses and the average $Q_{50\%}$ value of representative TS units are shown in Fig. 4. We found sharp tuning (e.g., units Y2, J3) as well as relatively broad frequency responses (e.g., unit M5). A few cells with two peaks in the frequency response (e.g., unit L5) were also present. Tuning in TS cells sometimes varied with level (e.g., unit M5). In addition, some cells exhibited level-dependent activity during particle motion stimulation: the response of the cell decreased as the stimulus level increased (Figs. 4B, E). The spike rate of Cell L6 (Fig. 4F) was suppressed below its background activity by all but the lowest level of auditory stimulation.

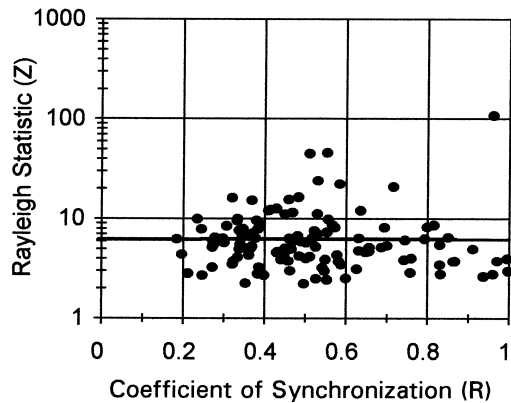


Fig. 5 Significance of phase-locking among cells in the torus semicircularis, as determined by the Rayleigh statistic (Z). The coefficient of synchronization (R) was calculated (see text) for each stimulus direction and level to assess phase-locking among all cells in the torus semicircularis. The line shown indicates the Z value above which phase-locking is unlikely to be a random event ($P=0.001$). Of 122 units plotted, 33% had significant phase locking in at least one direction and one signal level. No units were phase-locked at more than one level or more than one direction

Overall, 90 of 113 units (80%) exhibited monotonic rate-level functions, 12 (11%) of the units exhibited decreased activity with auditory stimulation, and 9 units (8%) showed more than one peak in the frequency response functions.

Phase-locking (the tendency for spikes to occur consistently at particular phases of a sinusoidal stimulus) was present in a subset of the midbrain cells (Fig. 5). We calculated the coefficient of synchronization (R) to assess phase-locking (R ranges from 0 to 1.0 for perfect phase-locking; Goldberg and Brown 1969). We used the Rayleigh Statistic ($Z=nR^2$, where n is number of spikes) to assess the statistical significance of those measurements for 122 TS cells. For each unit, we recorded the maximum Z value that occurred during the directional selectivity measures (at 100 Hz) over all signal levels and directions used. Using a highly conservative approach, we found that approximately one-third of the cells had maximum Z values that indicated significant phase-locking ($P < 0.001$ that what appears to be phase-locking is actually random activity) (Batschelet 1981). However, in no case was phase-locking consistent over the several signal levels and directional axes presented.

Directional responses

TS units were evaluated for their DRPs in the horizontal and mid-sagittal planes. Of 109 units evaluated, all were directional in at least one plane, and 73 (67%) had sharpened DRPs in at least one plane, as described for cells in the descending octaval nucleus previously (Fay and Edds-Walton 1999). We have called these "sharpened" cells because the spike rate maximum was much greater at the best direction than at adjacent directions (plus and minus 30°), giving the DRP a sharper outline

than the more rounded DRP of primary saccular afferents (Fay and Edds-Walton 1999). Sharpened DRPs are illustrated in Fig. 6. The cell in Fig. 6C is the most highly sharpened in the horizontal plane among these examples.

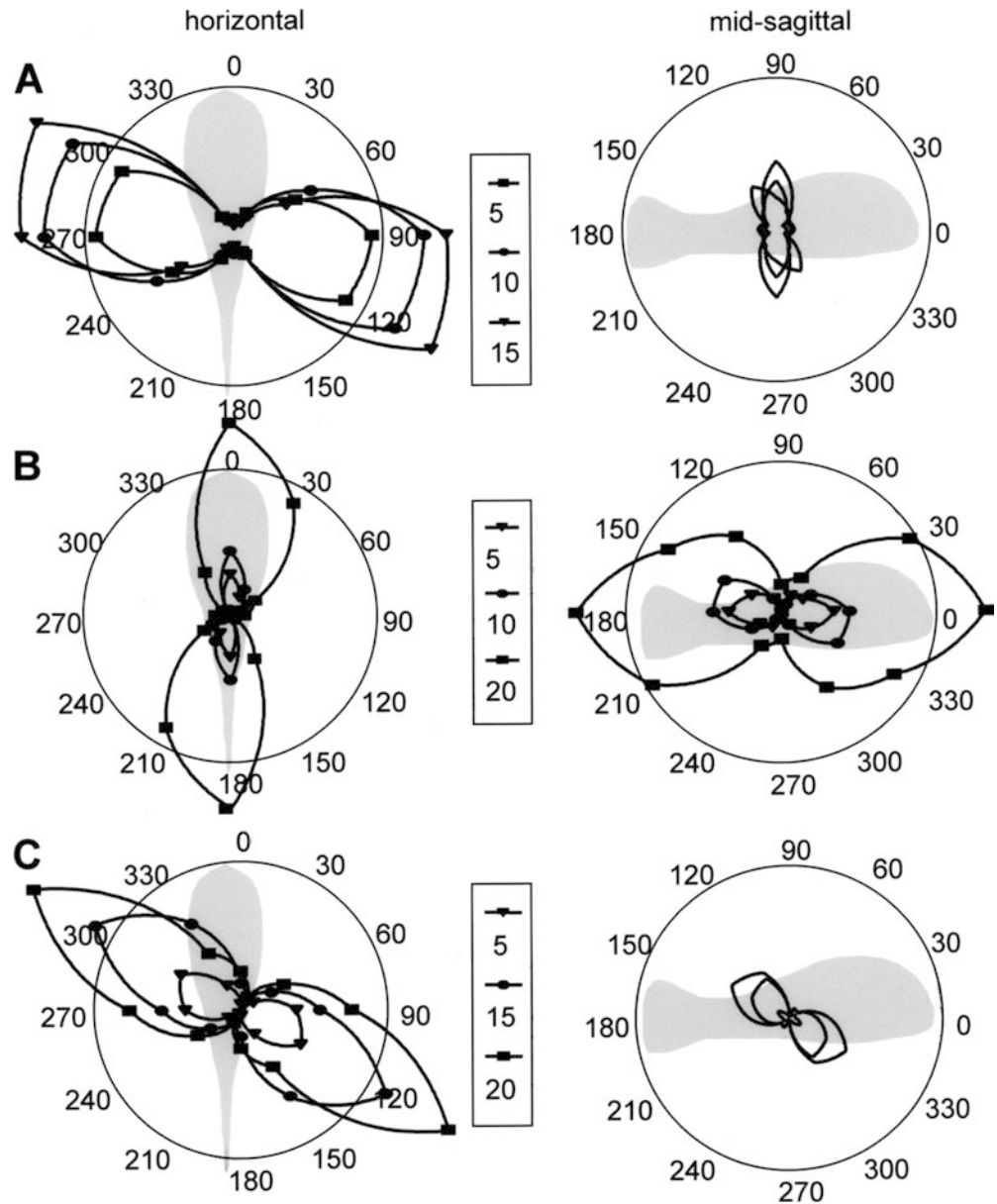
To obtain a quantitative representation of sharpening, we devised a "sharpening ratio". The sharpening ratio is the average spike rate at angles adjacent to the best direction (plus and minus 30°) divided by the spike rate at the best direction. For the cell illustrated in Fig. 6A, the sharpening ratio is the average of the spike rate at the $90-270^\circ$ and $150-330^\circ$ axes divided by the spike rate along the $120-300^\circ$ axis. The sharpening ratio ranged from 0.01 to 1 (for a response that is equivalent at three stimulus angles). A ratio of 0.87 corresponds to that expected from a cosine function, as generally found in primary saccular afferent responses. The average sharpening ratio for midbrain cells was 0.44 (s.d. ± 0.12 ; $n=87$) (Fig. 7). Our most highly sharpened cell had a sharpening ratio of 0.07. Six of the cells with consistent DRPs (7%) were not sharpened (ratio > 0.75).

Given that directional sharpening and frequency tuning in the TS are likely to be the result of inhibitory interactions, we looked for covariation in measures for sharpening and tuning. We plotted the sharpening ratio versus the $Q_{50\%}$ for all auditory cells (Fig. 8). A straight line would result if the two were related, but there is no evidence of any relationship between these two characteristics.

Unusual DRPs are illustrated in Fig. 9. The response illustrated in Fig. 9A is particularly interesting. The DRP at the lowest level shown (-10 dB re 1 nm) is nearly circular, and it has the highest spike rates. At higher stimulus levels (0 dB and above), the DRP contracts monotonically and begins to take on a directional orientation, particularly in the mid-sagittal plane. We interpret a directional DRP here as resulting from inhibition by a directional input. We infer that the inhibitory input was from a cell responding best (causing maximum suppression) on the horizontal plane, and having a null plane (causing minimal suppression) oriented vertically and passing through the rostro-caudal axis of the animal. Twelve percent (13/109) of TS units exhibited suppression of activity throughout their dynamic range.

Some cells had more than one best axis of motion in a single plane (e.g., Fig. 9B, horizontal axis). This sort of DRP pattern could result from multiple units recorded or from excitatory convergence of two differently oriented cells in the brain. There were 10 units (9%) with similar, multi-peaked DRPs observed in at least one plane. Of these, two also showed multiple peaks in the frequency response functions (as in Fig. 4, panel E), which is consistent with recording from two or more units simultaneously. However, the data in Fig. 9B were not likely to be from a multi-unit recording as the spike height was unusually large and uniform in level. Based on the sharpened appearance of both peaks in the horizontal plane for that cell, we believe the cell demonstrates

Fig. 6 Samples of typical, sharpened directional response patterns (DRPs) among three cells (A–C) in the torus semicircularis of the toadfish (*Opsanus tau*). The response (spikes s^{-1}) is shown for three stimulus levels represented by different symbols for the horizontal and mid-sagittal planes for each cell. Symbols are not used where the response varied little with level (mid-sagittal plane, A and C) to simplify the figure. The front-back stimulus is 0–180° in these plots. The best directions in each plane, the sharpening ratio, and the background activity for each: **A** P3-00, azimuth 280°, elevation 90°, sharpening ratio = 0.41, background activity 2.5 spikes s^{-1} ; **B** P1-01, azimuth 5°, elevation 0°, sharpening ratio = 0.46, background activity 0.5 spikes s^{-1} ; **C** P2-01, azimuth 330°, elevation 325°, sharpening ratio = 0.37, background activity was zero



excitatory convergence of inputs from two cells that had been sharpened prior to their convergence in the TS. This sort of excitatory convergence was rare in our data set.

Some units had little or no directional selectivity at any of the levels investigated. The recording site for the nondirectional unit in Fig. 9C was injected with neurobiotin and was in a cell group directly lateral to the lateral lemniscus in the midbrain. This site may have been a midbrain nucleus of the lateral lemniscus, as illustrated in trout by Nieuwenhuys and Pouwels (1983). Four other units that were not labeled (4%) showed similar, non- or omni-directional DRPs.

Another class of DRPs (not shown) was described as “irregular” (8/109 units or 7%). These cells exhibited DRPs in both planes that appeared to have multiple peaks, but the angles at which the peaks occurred tended to vary with level in ways that could not be

simply described or understood. These patterns could possibly have been caused by excessive spike rate variability.

Since the directional stimuli were all presented at 100 Hz, we examined the frequency responses of the cells without sharpening or with irregular DRPs to determine whether these cells tended to have a BF significantly above or below 100 Hz. The distribution of BFs for cells without sharpening or with irregular DRPs was not substantially different from the distribution of BFs for cells with well-defined DRPs in both planes. In fact, the majority of cells with nonsharpened DRPs had a BF of 84 or 100 Hz (22/31 = 73%). Therefore, we conclude that the frequency of the directional stimuli did not affect the DRPs that we obtained.

The best axis for 106 directional TS cells can be illustrated in spherical space as an axis that penetrates

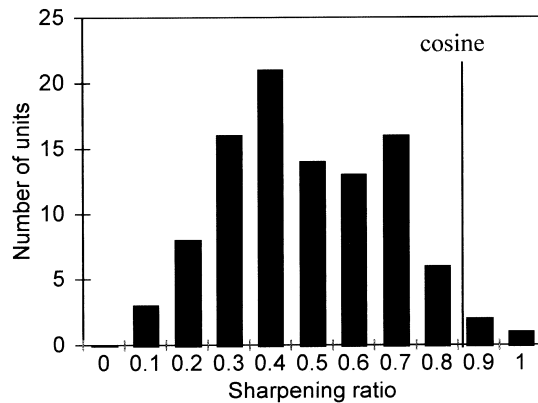


Fig. 7 Directional sharpening among cells in the torus semicircularis, represented by the sharpening ratio: average of spike rates at the adjacent angles ($\pm 30^\circ$ of the best direction)/spike rate at best direction. A ratio of 0.87 corresponds to the value expected for a cosine function (indicated by *vertical line*), as found in primary saccular afferents (Fay and Edds-Walton 1997a, Edds-Walton et al. 1999). Only a single sharpening ratio is given for each cell, which is the lowest ratio for the best direction in either the horizontal or the mid-sagittal plane

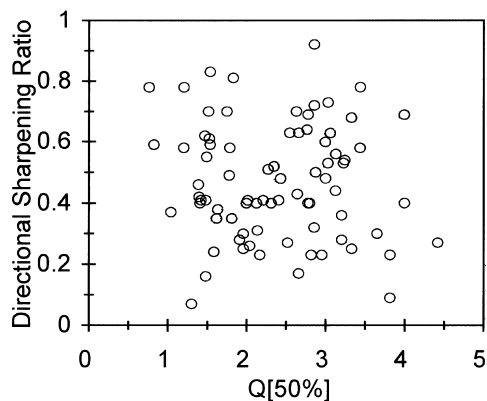


Fig. 8 Sharpening of the directional response versus the frequency tuning in auditory cells of the torus semicircularis in the toadfish. Directional sharpening is quantified as a sharpening ratio: average of spike rates at the adjacent angles ($\pm 30^\circ$ from the best direction)/spike rate at the best direction. Frequency tuning is quantified as $Q_{50\%}$: BF/BW is the frequency range at a spike rate 50% of the maximum at BF

the northern hemisphere of a globe (Fig. 10). Translational, oscillatory motion along an axis represented by each symbol is most effective in evoking spikes for a particular cell in our data set. We have represented the northern hemisphere here arbitrarily, as each best axis would penetrate the globe's surface in both the northern and southern hemispheres, but it is impossible to determine which end of the axis is the most excitatory.

The azimuths and elevations of these best axes vary widely among TS units, and no azimuth, elevation, or combination of the two appears improbable. There are axes that are essentially vertical (near the north pole), and others that lie on the plane of the equator in all quadrants. Although there is a continuous distribution of elevations between 0° and 90° , there is a substantial

number of cells with best elevations above 75° (see Discussion).

Bimodal units

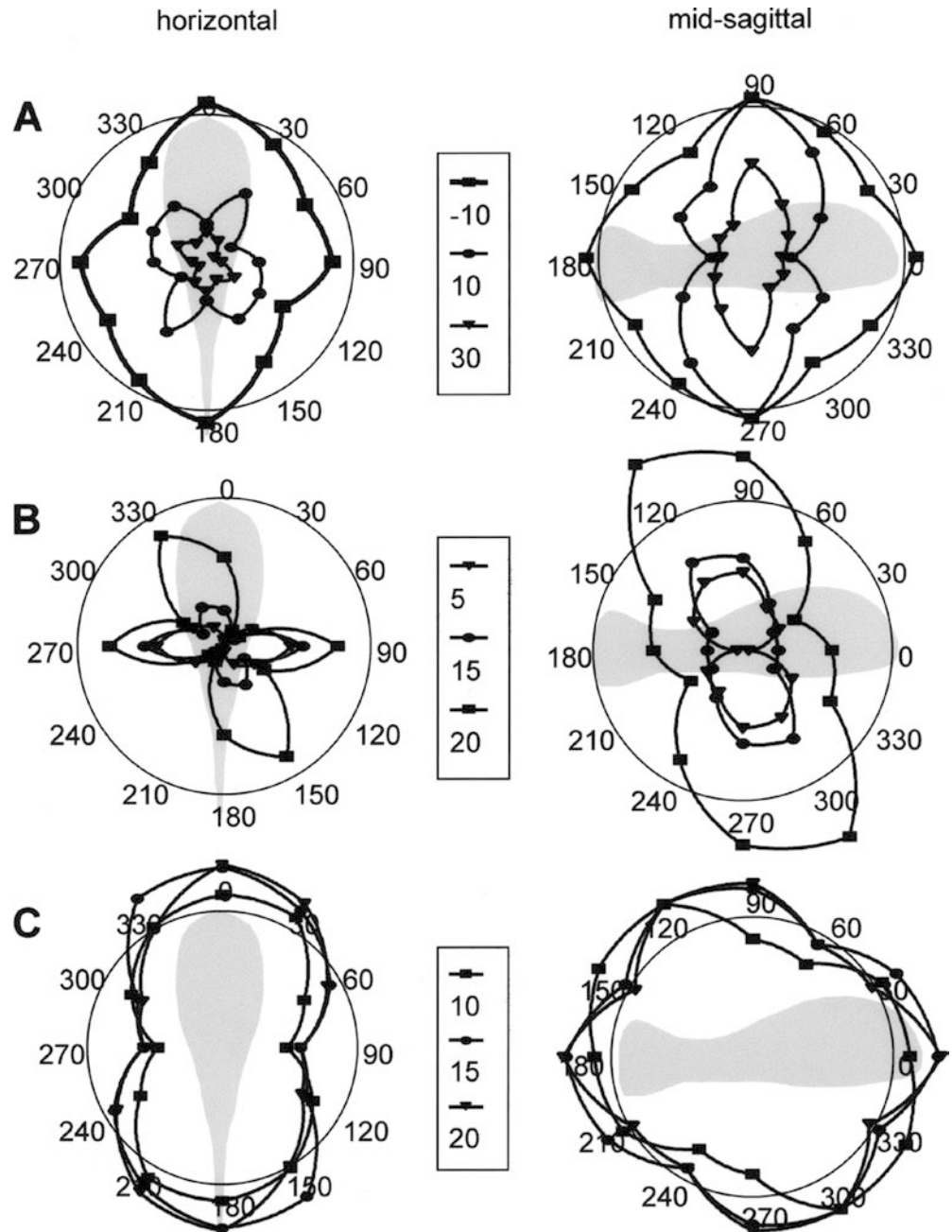
Light did not stimulate any of the units we tested, but many of the units in the TS ($n = 39$) responded to both the particle motion of our auditory stimuli and the noisy hydrodynamic stimulus. We classified these units as bimodal in a preliminary study (see Fay and Edds-Walton 2001). The additional data we have gathered is consistent with our original hypothesis that the cells are receiving input from both auditory and lateral line receptors. Although we were unable to determine thresholds or tuning with a series of lateral line stimuli, we feel it is important to describe these results to stimulate further research directed at confirming the receptors and quantifying the response characteristics in the midbrain.

Most bimodal units exhibited increases in spike rate with both auditory and hydrodynamic stimuli, although a few exhibited suppression. To quantify relative responsiveness to the hydrodynamic stimulus, we subtracted the average background activity (recorded prior to stimulation) from the average spike rate recorded during the hydrodynamic stimulus presentations. The average spike rates of 17 bimodal TS units to the hydrodynamic stimulus have been plotted to illustrate both ipsilateral and contralateral responsiveness (Fig. 11). The recording locations for all cells included in the figure were injected with neurobiotin and were in NC or NVL. The majority of bimodal cells responded to both ipsilateral and contralateral hydrodynamic stimulation, with some contralateral predominance. An example of a cell whose activity was suppressed by the hydrodynamic stimulus is also illustrated in Fig. 11 (cell 1). The background activity of that cell was equally suppressed by ipsilateral and contralateral hydrodynamic stimuli. A third type was excited by the hydrodynamic stimulus, but that response was inhibited by auditory stimuli (see section on suppressed cells).

We plotted the locations of bimodal cells versus the cells that responded only to the auditory (particle motion) stimulus based on the *in vivo* measurements using the 3-D micromanipulator. We have shown those cells as filled diamonds in Fig. 12. However, we caution that this plot is only intended to illustrate the relative distribution of the recording sites in the TS, as the size and shape of NC and NVL are not consistent throughout their extent in the midbrain. No recording sites are located at the most extreme lateral-medial locations of these plots because the sites were plotted with respect to the edges of the tectal surface. Surface area of the TS is considerably smaller than that of the optic tectum (approximately only 60%).

There is no clear trend with regard to depth (Fig. 12A), although the plot is consistent with an overlap in the distribution of bimodal and auditory-only

Fig. 9A–C Unusual directional response patterns from three cells in the midbrain of the toadfish. **A** The background activity of K1-00 was suppressed by the particle motion stimulus (azimuth 340°, elevation 85°, BF 84 Hz, background activity 4.3 spikes s⁻¹). **B** Cell G2-01 may have had two excitatory inputs (azimuth double-peaked, elevation 112°, BF 84 Hz, background activity 1.5 spikes s⁻¹). **C** Cell H1-01 was nearly omnidirectional and was located adjacent to the lateral lemniscus (BF 100 Hz, background activity 8.8 spikes s⁻¹)



cells. The deepest bimodal cell was suppressed by auditory activity (T1, Table 1). The data clearly indicate that bimodal cells are scattered throughout the rostral-caudal extent of the TS, and they tend to be more lateral in the most rostral locations (Fig. 12B).

Our initial injection site analyses indicate that bimodal cells may be located in both NC and NVL (P.L. Edds-Walton and R.R. Fay, unpublished observations). Cells with relatively large somas and extensive arborizations in NVL and NC were filled by our neurobiotin injections in the TS (Fig. 13). We suspect that these cells may be bimodal units. The large size of the soma also would explain the relative ease with which we located bimodal cells and obtained excellent extracellular spike definition from them during this study. The periventricular cells

(PVC layer) in the TS also have long processes that traverse the NC or the NVL, (see Fig. 13A, B, this paper; Bass et al. 2000) and groups of those cells were filled in nearly all cases of neurobiotin injection. While these small cells may also integrate toral inputs, they are not likely to be the cells from which we were recording bimodal responses. The label site was always ventral of the PVC layer, and we think it highly unlikely that we were recording from their dendrites.

Suppression

Activity was inhibited in some TS cells by auditory input, resulting in a decrease in spike rate as the stimulus

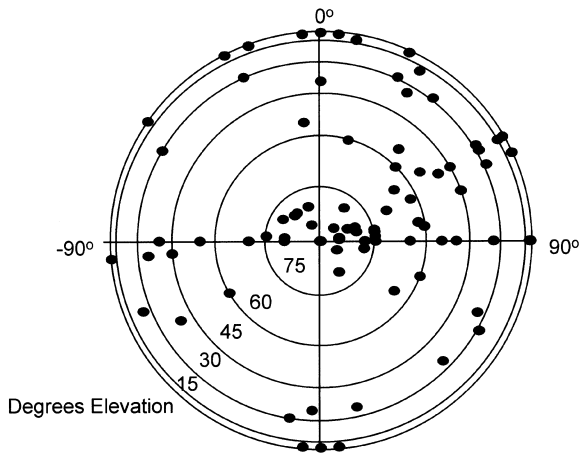


Fig. 10 Best direction for 106 directional cells from the TS of the toadfish. Note that cells from both nucleus centralis and nucleus ventrolateralis are included as no obvious differences were apparent in the distribution of their best axes. The data are plotted as if on the northern hemisphere of a globe, with the fish at the center. Azimuth is represented radially (0° at the fish's head). Elevation is represented by the *concentric circles*, with 90° in the center. Each *symbol* represents the location on the globe's surface where the best direction (best azimuth and best elevation) of a single unit penetrates the northern hemisphere. Translatory motion along that axis is most effective in evoking spikes for each cell represented

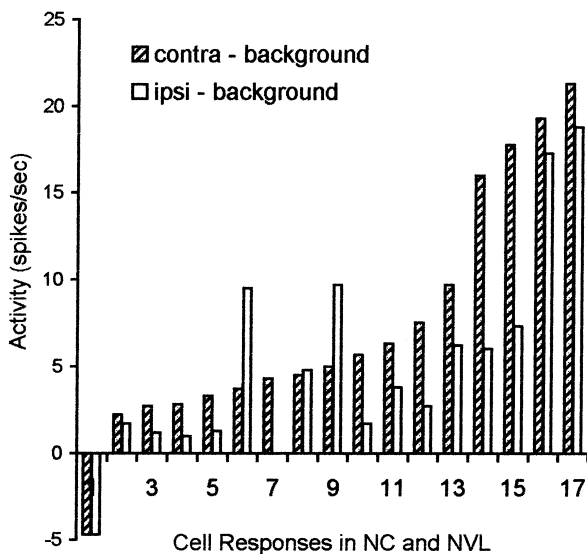


Fig. 11 Spike activity in bimodal units in response to hydrodynamic stimulation, ipsilaterally and contralaterally to the recording site in the torus semicircularis of the toadfish. The locations of all units were confirmed by identification of the neurobiotin injection site. Each *bar* represents the evoked spike rate minus the background activity recorded prior to hydrodynamic stimulation. The background activity of cell 1 was suppressed by the hydrodynamic stimulus, ipsilaterally and contralaterally. *contra* contralateral; *ipsi* ipsilateral; *NC* nucleus centralis; *NVL* nucleus ventrolateralis

level increased (e.g., Figs. 4F, 9A). Sites where a unit's activity decreased with auditory stimulation tended to be located deeply in the TS (e.g., circle in Fig. 1B). Therefore, we compared the depths of suppressed/inhibited

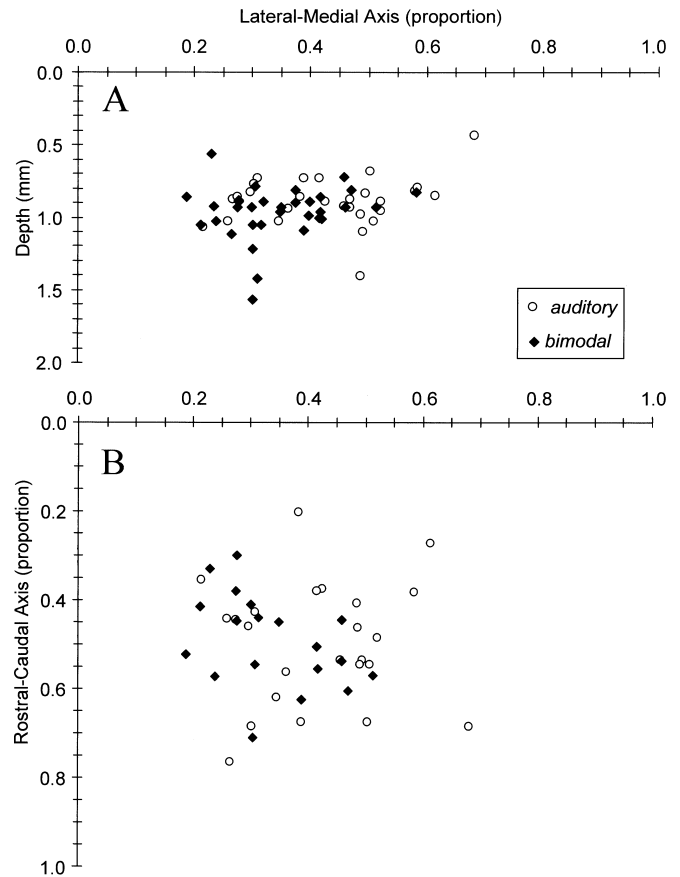


Fig. 12A,B Locations of sites with bimodal responses (*filled diamonds*) versus auditory-only sites (*open circles*) from in vivo measurements. **A** Depths were obtained by subtracting depth of recording site from the surface measurements (on the optic tectum) and, therefore, included the tectal thickness and the ventricular space. Each site was plotted with respect to the percentage distance from the lateral edge to the medial edge in each fish to control for differences in size and shape of the optic tectum among fish. **B** Recording sites plotted by rostral-caudal and lateral-medial locations. Note that bimodal sites were located all along the rostral-caudal axis. All 3-D measurements were not recorded for some sites; therefore the number of sites in each plot differs slightly

cells with the depths of nonsuppressed cells in the same individuals (Table 1). On average, the suppressed/inhibited cells were significantly deeper ($n=9$ fish, 10 cells exhibiting auditory suppression, 13 nonsuppressed cells; $P < 0.008$, *t*-test, single tail, for data with unequal variances). The BFs for suppressed cells were all at 100 Hz or below, as defined by the most suppressive frequency.

Some of the cells suppressed by auditory stimuli could be excited by the hydrodynamic stimulus. For example, unit K1 (2001) in the NVL had a background rate of 2.5 ± 2.6 spikes s^{-1} (mean \pm s.d.). K1 was excited by hydrodynamic stimulation (cell 9 in Fig. 11). In the presence of simultaneous hydrodynamic stimulation and a directional auditory stimulus (side-to-side, 100 Hz at 20 dB re: 1 nm), cell K1 activity was maximally suppressed to 1.3 ± 0.97 spikes s^{-1} . Cell Z1 (2001) is another example of a cell in NVL that responded to the

Table 1 Depth comparison for suppressed cells and nonsuppressed cells recorded in the same toadfish. The depths were measured in vivo with respect to the optic tectum. The letter identifies the fish; the number identifies the cell

Suppressed cells		Depth (mm)	Nonsuppressed cells		Depth (mm)
L	6	1.01	L	1	0.89
N	3	1.39	L	4	0.74
T	1	1.57	N	1	1.04
T	4	1.22	N	2	1.04
W	1	1.05	T	3	1.05
X	1	0.93	W	2	0.56
Y	1	0.835	X	3	0.72
Z	1	0.93	Y	2	0.93
aa	4	0.92	Z	2	0.86
aa	5	1.12	Z	4	0.96
			Z	5	0.74
			aa	2	0.81
			aa	3	0.9
Mean		1.10	Mean		0.86
s.d.		0.23	s.d.		0.15

Statistics: *t*-test: one tailed, two-sample assuming unequal variances; *df*=14; *t*stat=2.7614; $P(T \leq t) = 0.0076$

hydrodynamic stimulus (cell 11 in Fig. 11) but whose activity was suppressed by auditory input. The average background activity was 9.5 ± 2 spikes s^{-1} ; however, with a directional particle motion stimulus at 20 dB (re 1 nm), the activity was suppressed to 0.5 ± 1.2 spikes s^{-1} .

Lastly, we obtained two cases in which a cell's responses to auditory stimulation were inhibited by the simultaneous presentation of the hydrodynamic stimulus. For example, cell Z2-01 responded to a 12 dB (re: 1 nm) directional, shaker stimulus (at 100 Hz) with an average of 15.8 ± 4.6 spikes s^{-1} . When a hydrodynamic stimulus was presented ipsilaterally simultaneously with the same shaker stimulus, the cell's average activity decreased to 2.8 ± 2.4 spikes s^{-1} .

Responses at sites labeled with neurobiotin

A single recording site was labeled with neurobiotin in 34 fish following physiological characterization of a unit. The locations of the recording sites were compared among fish in the following way. The shape and size of NC and NVL vary rostro-caudally in the toadfish. Therefore, the recording locations labeled with neurobiotin were grouped by their rostro-caudal location to determine whether they were in NC, NVL, or the DCL that lies below NVL.

A brain with extensive label throughout the NVL was used as a template for approximating the borders of NVL throughout the TS. Then recording locations were plotted as caudal, middle, or rostral TS using the following landmarks. Caudal toral sites were assigned based on the presence of the lateral lemniscus, the caudal, diffusely organized hypothalamus, and small torus longitudinali. The most caudal sites were rostral of the valvulae of the cerebellum. Middle toral sites were

defined as those wherein the lateral lemniscus was clearly evident and the hypothalamus was present. Rostral toral sites were defined as those sites in sections rostral of the formation of the lateral lemniscus, with nucleus diffusus and nucleus glomerulosus present.

The physiological data were compared based on the rostral-caudal groupings and medial-lateral location. The only physiological correlates were associated with the location in the functional subdivisions of the torus. Therefore, the data will be presented by these regions of the torus: NC, NVL or the DCL, or near the apparent ventral border for NC (NC/NVL). Fourteen units were located in NC, 11 units in the NVL or the deep cell layer, and 6 were near the NC/NVL border. Those border cells could not be assigned with certainty to either nucleus since the NC/NVL border is not distinct in *Opsanus* (Bass et al. 2001). The few sites in the deep cell layer were included with NVL since there is no distinct border for NVL and DCL, and all of those cells responded to the hydrodynamic stimulus. One injection site was in a cell group adjacent to the lateral lemniscus, which may have been a nucleus of the lateral lemniscus as illustrated by Nieuwenhuys and Pouwels (1983) in the trout. Two injections were too large to permit identification of the recording site.

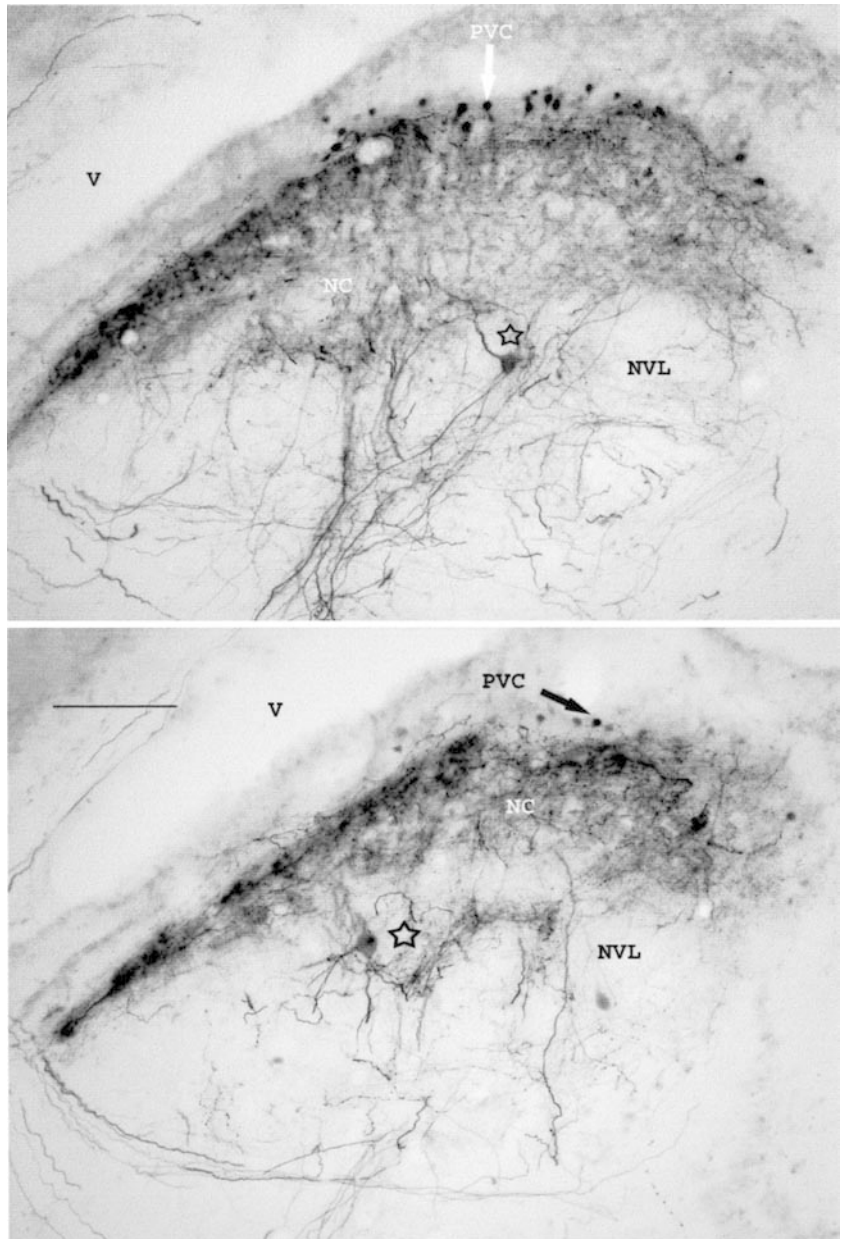
Frequency-tuned NC units tended to have higher BFs than units in NVL (NC mean BF = 104 Hz; NVL mean BF = 78 Hz). A one-tailed *t*-test (assuming unequal variance) indicated these differences were significant ($P = 0.014$; $n = 20$; *df* = 14). The variation among BFs of the units at the NC/NVL border was very high (range 50–141 Hz), and there was no statistical significance to BF comparisons with NC or NVL. This result is not unexpected since it is likely there was a mixture of NC and NVL cells in this border category.

We investigated the potential role of lateral line input to directional analyses by comparing the sharpening ratios for cells in the NC versus those in NVL. Border cells were not included in these analyses. As noted earlier (see Directional responses), the mean sharpening ratio was 0.440 for the entire data set. The mean sharpening ratio for NC cells was 0.561 in the vertical plane and 0.396 for the horizontal plane. The mean sharpening ratio for NVL cells was 0.448 in the vertical plane and 0.348 in the horizontal plane. These data indicate that there are cells in both divisions of the TS that process directional information, and sharpening is present in both divisions. A detailed description of the locations of the recording sites and the cells filled retrogradely after injections in the TS will be presented in a subsequent publication.

Discussion

Background activity (defined as activity in the absence of our stimuli) was under 3 spikes s^{-1} for the majority of cells of the TS, unlike primary saccular afferents. We found background rates well over 100 spikes s^{-1} in the

Fig. 13 Filled cells in NVL. Note that both multipolar cells (*open stars*) have relatively large cell bodies with processes that extend dorsally into NC and ventrally within NVL. The axon of the upper cell travels medially, but the actual projection site was not detectable. Scale bar = 100 μm (*lateral is left, dorsal is up; PVC* periventricular cell, *V* ventricle)



periphery (Fay and Edds-Walton 1997a). Little background activity has been reported for TS sites in other fish species, including goldfish (Lu and Fay 1993; Ma and Fay 2002) and the weakly electric fish *Pollimyrus* (Crawford 1993; Kozloski and Crawford 1998).

Phase-locking, or the tendency for an afferent to produce a spike at a particular phase of a sinusoidal stimulus, was strong in saccular afferents (Fay and Edds-Walton 1997a), weak in the DON (P.L. Edds-Walton and R.R. Fay, unpublished observations), and relatively uncommon in the TS of toadfish (this study). The values for the coefficient of synchronization (R) among TS cells varied widely, but about one-third of the cells exhibited statistically significant phase-locking (Fig. 6). Phase-locking was not robust, however, in that the response was never consistent across signal levels or

directional axes. This is potentially important in that these cells may be encoding particular combinations of phase, direction, and signal level.

Phase-locking has been reported in the TS of a few other teleosts. In goldfish, Lu and Fay (1993) found a subset of midbrain units that were described as strongly phase-locked. In *Pollimyrus*, Crawford (1993) reported that only about 10% of the cells that responded to tones exhibited phase-locking. Schellart et al. (1987) found both phase-locking and relatively high spontaneous activity (up to 50 spikes s^{-1}) in a subset of cells in the TS of rainbow trout; however, they also suspected that they may have recorded activity from medullary axons. Overall, previous studies indicate that phase-locking is present in a subset of TS cells in teleosts from different taxonomic groups. Our data indicate that these cells may

be components of the directional auditory circuit in the CNS of toadfish, but cells that do not phase-lock are equally directional.

Frequency response

The range of BFs in the TS of the toadfish is consistent with our previous work on saccular afferents (Fay and Edds-Walton 1997b) and cells of the DON (Fay and Edds-Walton 2000). However, the distribution of BFs differs in the DON and in the TS. Approximately 35% of the DON cells from which we recorded had a BF of 185 Hz, and only 5% (6/109) of all TS cells had a BF of 185 Hz. Fay and Edds-Walton (2000) suggested that the differences in BF distributions for these two levels of the auditory system may represent sampling error, since their preliminary findings were based on 92 DON cells and 24 TS cells. The additional recordings in the TS that we report here have not revealed a higher proportion of the higher-frequency BFs. Instead, a greater proportion of cells with BFs of 84 and 100 Hz was found.

There are two potential reasons for the differences in BF distributions of the DON and the TS. First, and most likely, our sample of TS cells includes both the NC and the NVL. Our comparison of BFs for injected sites in the NC versus the NVL indicates that the cells in the NC have higher BFs on average than NVL cells. None of the NVL cells had a BF above 100 Hz. Our sample set may have been biased to lower frequencies, given our attempts to document the locations of bimodal cells, which were primarily in NVL.

The second possibility is that there are frequency maps in DON and/or the TS, and we did not sample all sites uniformly to obtain a representation of all the frequencies. Echterler (1985) observed a crude tonotopy in the goldfish midbrain. Schellart et al. (1987) suggested that there are high-frequency and low-frequency areas in the TS of a trout, an auditory generalist like the toadfish. High frequency cells in trout responded only to frequencies above 125 Hz and were most often found in the rostral TS. The BFs of all our injected cell sites were compared, and there was no obvious map of frequency beyond the distinction between NC and NVL noted above. The high frequency cells of Schellart et al. (1987) may be equivalent to our auditory-only cells in NC. Our cells with best frequencies of 141 Hz were most common in the rostral NC, and none were observed in the caudal NC. While these data are suggestive, we feel our data set is too small to offer definitive evidence on whether or not a frequency map exists along the rostral-caudal axis of NC in toadfish. Additional data are needed to test the frequency map hypothesis.

The most common BFs are consistent with the frequencies in the first harmonic of the reproductive boatwhistle call of *O. tau* at the temperature range in which the experimental animals are found. The boatwhistle is composed of rapidly produced pulses of sound. The pulse repetition rate is temperature dependent

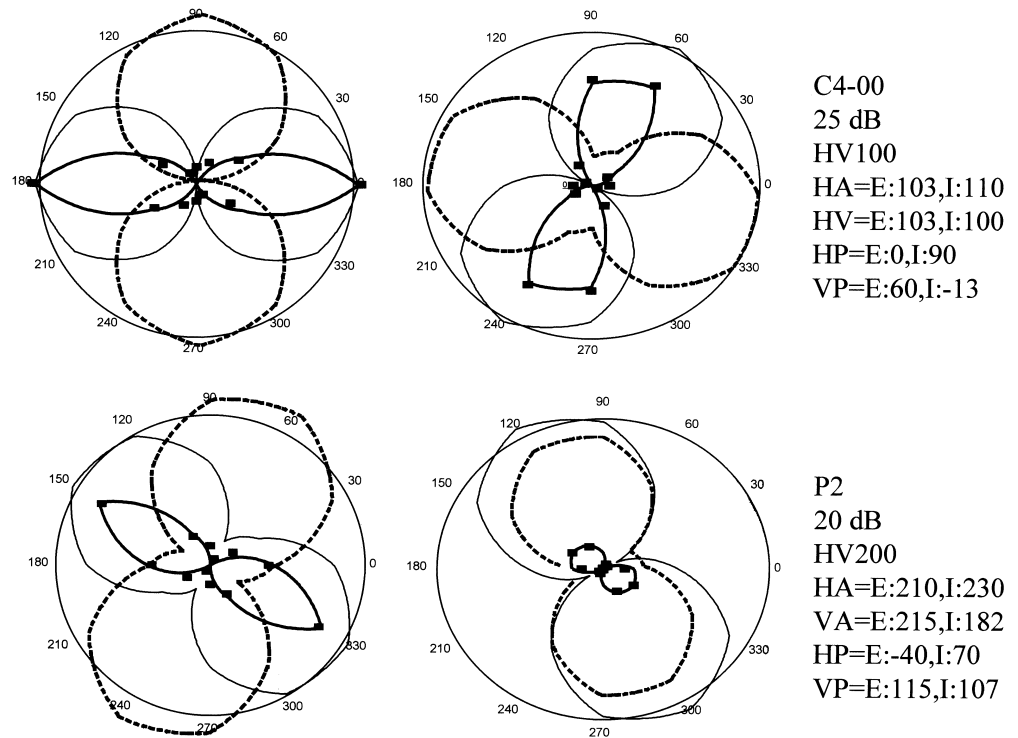
(Bass and Baker 1991), but the rate also varies among individuals at the same temperature (Edds-Walton et al. 2002). The first harmonic in the boatwhistle produced by toadfish in the Woods Hole, MA area is about 125–160 Hz early in the breeding season when water temperatures are below 20°C. Later in the breeding season, as water temperature increases above 20°C, the first harmonic is about 200 Hz. Although our data from the TS indicate that the toadfish auditory system has a majority of fibers tuned to the frequencies that occur early in the breeding season, our data from the medulla (Fay and Edds-Walton 2000) indicate that toadfish can hear the first harmonic across the normal range of temperatures during the breeding season. Since all of the fish used in this study of the TS were obtained between June and July, we cannot address the issue of seasonal changes in frequency response, as reported by Sisneros and Bass (2003) for *Porichthys notatus*.

Frequency responses varied widely among TS cells, including relatively narrow tuning (e.g., Y2) not seen in the periphery. The reverse correlation method was used previously to characterize the frequency response of saccular afferents (Fay and Edds-Walton 1997b, Edds-Walton et al. 1999). Overall, saccular afferents had broadband response characteristics. The range of tuning seen in the TS indicates that there is a range of inhibitory interactions that sharpen the frequency responses seen in the periphery. In some cases, the sharpening is level dependent (e.g., Fig. 4D, E). In goldfish, auditory mid-brain units show a wide variety of frequency response areas, including multi-peaked and discontinuous areas, and “island” areas that close up at the highest stimulus levels (Lu and Fay 1993). These are most likely due to inhibitory processes at or below the midbrain level from primary-like inputs with very different best frequencies. Those frequency response areas were not observed in the toadfish midbrain. Inhibition from cells having a best frequency near that of the excitatory input would be expected to truncate or sharpen an excitatory frequency response area in oyster toadfish, but would not be expected to sculpt the complex shapes observed in goldfish.

Directional responses

The majority of the auditory units obtained in the TS during this study were directional and sharpened (67%), responding best to a particular axis of particle motion stimulation. Sharpening has been explained with the following simple model, originally described for cells in the descending octaval nucleus by Fay and Edds-Walton (1999) and also applied to TS cells in goldfish by Ma and Fay (2002): The unit recorded from receives at least two inputs assumed to be cosinusoidally shaped (similar to primary afferent units and some units found in the descending octaval nucleus; P.L. Edds-Walton and R.R. Fay, unpublished observations). One input is excitatory and one inhibitory (Fig. 14). In the model, spike rates predicted to be negative were set to zero. In this case, the

Fig. 14 Demonstration of the sharpening model. One excitatory input (*solid thin line*) and one inhibitory input (*dashed line*) are shown for cell C4-00 (at 25 dB) and cell P2-01 (at 20 dB). The addition of the excitatory and inhibitory inputs would result in the sharpened directional response pattern shown with the heavier line. *Square symbols* are the data to be modeled (see Fay and Edds-Walton 1999). *E* excitatory, *HA* horizontal amplitude, *HP* horizontal phase, *HV* horizontal phase, *HV* maximum radial axis (*circle*) in both planes, *I* inhibitory, *VA* vertical amplitude, *VP* vertical phase



sum of two cosinusoidal inputs with opposite sign always produces a resultant that is sharpened to some degree. The shape, size, and directional orientation of the resultant is a function of the angles and magnitudes of the two hypothetical inputs. Fig. 14 illustrates this sort of interaction for two TS units: C4-00 and P2-01 in the horizontal and mid-sagittal planes. In each of the four panels, polar plots show the observed data for a sharpened unit (symbols) and the model (dark solid lines) that was best fit by eye. The model was computed by subtracting the hypothetical inhibitory cosine function (dark, dashed lines) from the hypothetical excitatory cosine function (thin, solid lines). In each of these cases, this model fits the data reasonably well.

Given that both sharpening and frequency tuning can be achieved by inhibition that narrows the responsiveness of the cell, we looked for a relationship between the directional sharpening ratio and $Q_{50\%}$, the measure of frequency tuning (Fig. 8). Our data indicate that the two processes (frequency tuning and directional response sharpening) are independent in the TS.

The site of inhibitory and excitatory interactions that result in sharpening may be the TS, but our data from the DON indicate that many of the cells there are sharpened (Fay and Edds-Walton 1999). In addition, the secondary octaval nuclei provide input to the TS, the nature of which is unknown. At this stage of our study, we cannot determine the source of the inhibitory input, but finding the source is of major importance for understanding the directional auditory circuit in these fishes.

Wubbels et al. (1995) found only 35% of their auditory units ($n = 183$) in the TS were directional, and their directional selectivity was variable. Although Wubbels

et al. (1995) reported that their auditory units were dorsal (within 800 μm of the surface of the TS), as are the units that we sampled, our use of a circular, directional search stimulus may have allowed us to be more successful in finding directional units. In addition, we tested both the horizontal and mid-sagittal planes, while Wubbels et al. (1995) and Wubbels and Schellart (1998) used only horizontal stimulation. Thus far, we have not been able to confirm the directional mapping reported by Wubbels et al. (1995) and Wubbels and Schellart (1998). We had few recordings along the same vertical track, but we did not find similar DRPs among cells along the same track when we were able to sample vertically.

The distribution of best axes in the left TS of the toadfish (Fig. 10) is in sharp contrast to the distribution of best axes in afferents from the left saccule. Edds-Walton et al. (1999) found that most left saccular afferents had a best azimuth about 290–300° to the left, which coincided with the orientation and curvature of the saccular endorgan with respect to the midline of the fish. No saccular afferents with elevations above 75° were observed. Cells in the TS have a wide range of azimuths and elevations, including a subset with elevations near 90°. Vertically oriented hair cells are present on the saccule, but they were not well represented in the data set obtained by Edds-Walton et al. (1999). Given the difficulty in accessing afferents that innervate the small area of the toadfish saccule where the vertically oriented hair cells are located (Edds-Walton and Popper 1995), we believe that limited sampling explains the difference in the range of elevations for saccular afferents versus TS cells.

Although we cannot eliminate the possibility that other endorgans are involved, the great range of best axes from the toadfish TS could be the product of computations (excitatory and inhibitory interactions) from the directional input of saccular afferents that we have documented. Based on the hair cell orientations on the saccule (Edds-Walton and Popper 1995), elevation could be obtained by comparison of responses across hair cells within a single saccule. In addition, based on physiological data, Edds-Walton et al. (1999) suggested that the toadfish could calculate azimuth by comparing the relative responsiveness of the left and right saccule, without input from other otolithic endorgans.

The data reported here indicate that all axes of acoustic particle motion (and all potential source locations) around the fish are probably represented in the TS. The majority of cells in both the NC and the NVL of the TS respond best to particle motion stimulation along a particular axis. The presence of a wide range of best azimuths on both sides of the fish is consistent with a convergence of directional information from the left and right ears. At present we do not know whether the TS is the site at which this convergence occurs. Neurophysiological recordings of directional response characteristics are needed in both the DON and the secondary octaval population in the medulla to determine the first site of binaural directional processing. This information is important for modeling directional hearing in fishes as well as modeling the evolution of directional hearing circuitry in vertebrates.

Bimodal cells

We believe that the bimodal cells have information from the lateral line and the auditory system for the following reasons: (1) the dominant frequencies in our hydrodynamic stimulus were below 10 Hz (Fig. 2); (2) our hydrodynamic stimulus excited lateral line afferents similarly to water jets (Tricus and Highstein 1990, and P.L. Edds-Walton and R.R. Fay, personal observations); (3) the most sensitive auditory cells did not respond to the hydrodynamic stimulus (Fig. 3); (4) relative responsiveness to the hydrodynamic stimulus and auditory stimuli was variable (Fig. 11), including inhibition by either stimulus, which is also consistent with an interplay between two separate sensory systems; and (5) large, multipolar cells with processes in both the NC and the NVL are good candidates for the bimodal cells (Fig. 13).

Sites that responded to both the auditory stimuli and hydrodynamic disturbances were distributed throughout the rostral-caudal extent of the TS in the toadfish (Fig. 12). These bimodal cells could be receiving input from other unimodal cells in NC and NVL, or directly from ascending afferents from the medulla. Given the range of relative responsiveness we found to the two classes of stimuli, input from the two sensory systems can be either excitatory or inhibitory.

Additional recordings at identified sites are needed to determine the distribution of the cells with different bimodal responses.

The functional significance of bimodal responses is of particular interest in the context of sound source localization. One of the problems in understanding how fish locate a sound source in space has been unraveling how fish solve the 180° ambiguity inherent in oscillatory particle motion (e.g. Schuijf 1981). Oscillatory particle motion is a to and fro movement. Therefore, the particle motion axis alone will not provide sufficient information for the fish to distinguish a source in front from a source behind the fish, or a source to the left versus one to the right. Schuijf (1981) suggested that the gas bladder might be involved in directional sound analyses, but the gas bladder probably does not provide auditory input to the ears in toadfish (Yan et al. 2000). Input from the lateral line could provide unambiguous information about where the sound source lies (e.g., Coombs et al. 2000) if the sounds are of appropriate frequency and sufficient intensity (e.g., those below approximately 200 Hz, at close range to the toadfish).

Our evidence that directional sharpening is present in cells of the NVL indicates that the NVL may be an important component of brain circuitry designed to locate sources of acoustic as well as hydrodynamic signals. Sensory integration is thought to be a major role of the midbrain of vertebrates in general (Casseday and Covey 1996). For the toadfish, and perhaps all teleost fishes, sensory integration in the midbrain includes directional information from the auditory and lateral line systems.

Acknowledgements Both authors have been supported by grants from the NIH (DC03666). We thank E. Enos and A. Sexton for their assistance in obtaining oyster toadfish of the appropriate size for these experiments. We thank Lisa Mangiamele for her unflinching energy in providing assistance with portions of the histology during the busy summer of 2001. Sheryl Coombs provided helpful suggestions and the hot-film anemometer system to quantify the hydrodynamic stimulus. We also thank the two anonymous reviewers for their detailed comments that led to significant improvements in data presentation.

References

- Bass AH, Baker R (1991) Evolution of homologous vocal control traits. *Brain Behav Evol* 38:240–254
- Bass AH, Bodnar DA, Marchaterre MA (2000) Midbrain acoustic circuitry in a vocalizing fish. *J Comp Neurol* 419:505–531
- Bass AH, Bodnar DA, Marchaterre MA (2001) Acoustic nuclei in the medulla and midbrain of the vocalizing gulf toadfish (*Opsanus beta*). *Brain Behav Evol* 57:63–79
- Batchelet E (1981) *Circular statistics in biology*. Academic Press, New York
- Carr CE (1992) Evolution of the central auditory system in reptiles and birds. In: DB Webster, RR Fay, A N Popper (eds) *The evolutionary biology of hearing*. Springer, Berlin Heidelberg New York, pp 511–543
- Casseday JH, Covey E (1996) A neuroethological theory of the operation of the inferior colliculus. *Brain Behav Evol* 47:311–336
- Coombs S, Fay RR, Janssen J (1989) Hot-film anemometry for measuring lateral line stimuli. *J Acoust Soc Am* 85:2185–2193

- Coombs S, Finneran J, Conley R (2000) Hydrodynamic imaging by the lateral line system of the Lake Michigan mottled sculpin. *Philos Trans R Soc Lond Ser B* 355:1111–1114
- Crawford JD (1993) Central auditory neurophysiology of a sound producing mormyrid fish: the mesencephalon of *Pollimyrus isidori*. *J Comp Physiol A* 172:1–14
- Echteler SM (1985) Tonotopic organization in the midbrain of a teleost fish. *Brain Res* 338:387–391
- Edds-Walton PL (1998) Anatomical evidence for binaural processing in the descending octaval nucleus of the toadfish (*Opsanus tau*). *Hear Res* 123:41–54
- Edds-Walton PL, Fay RR (1998) Directional auditory responses in the descending octaval nucleus of the toadfish (*Opsanus tau*). *Biol Bull* 195:191–192
- Edds-Walton PL, Popper AN (1995) Hair cell orientation patterns on the sacculus of juvenile and adult toadfish, *Opsanus tau*. *Acta Zool* 76:257–265
- Edds-Walton PL, Fay RR, Highstein SM (1999) Dendritic arbors and central projections of physiologically characterized auditory fibers from the sacculus of the toadfish, *Opsanus tau*. *J Comp Neurol* 411:212–238
- Edds-Walton PL, Mangiamele LA, Rome LC (2002) Variations of pulse repetition rate in boatwhistle sounds from oyster toadfish (*Opsanus tau*) around Waquoit Bay, Massachusetts. *Bioacoustics* 13:153–173
- Fay RR, Edds-Walton PL (1997a) Directional response properties of saccular afferents of the toadfish, *Opsanus tau*. *Hear Res* 111:1–21
- Fay RR, Edds-Walton PL (1997b) Diversity in frequency response properties of saccular afferents of the toadfish, *Opsanus tau*. *Hear Res* 113:235–246
- Fay RR, Edds-Walton PL (1999) Sharpening of directional auditory responses in the descending octaval nucleus of the toadfish (*Opsanus tau*). *Biol Bull* 197:240–241
- Fay RR, Edds-Walton PL (2000) Frequency response of auditory brainstem units in toadfish (*Opsanus tau*). *Biol Bull* 199:173–174
- Fay RR, Edds-Walton PL (2001) Bimodal units in the torus semicircularis of the toadfish (*Opsanus tau*). *Biol Bull* 201:280–281
- Fay RR, Edds-Walton PL, Highstein SM (1994) Directional sensitivity of saccular afferents of the toadfish to linear acceleration at audio frequencies. *Biol Bull* 187:258–259
- Goldberg JM, Brown PB (1969) Response of binaural neurons of dog superior olivary complex to dichotic tonal stimuli: some physiological mechanisms of sound localization. *J Neurophysiol* 32:613–636
- Hancock MB (1982) A serotonin immunoreactive fiber system in the dorsal column of the spinal cord. *Neurosci Lett* 31:247–252
- Highstein SM, Kitch R, Carey J, Baker R (1992) Anatomical organization of the brainstem octavolateralis area of the oyster toadfish, *Opsanus tau*. *J Comp Neurol* 319:501–518
- Kozloski J, Crawford JD (1998) Functional neuroanatomy of auditory pathways in the sound-producing fish *Pollimyrus*. *J Comp Neurol* 401:227–252
- Lu Z, Fay RR (1993) Acoustic response properties of single units in the torus semicircularis of the goldfish, *Carassius auratus*. *J Comp Physiol A* 173:33–48
- Ma W-LD, Fay RR (2002) Neural representations of the axis of acoustic particle motion in nucleus centralis of the torus semicircularis of the goldfish, *Carassius auratus*. *J Comp Physiol A* 188:310–313
- McCormick CA (1989) Central lateral line mechanosensory pathways in bony fish. In: Coombs S, Görner P, Munz H (eds) *The mechanosensory lateral line*. Springer, Berlin Heidelberg New York, pp 155–217
- McCormick CA (1992) Evolution of central auditory pathways in anamniotes. In: Webster DB, Fay RR, Popper AN (eds) *The evolutionary biology of hearing*. Springer, Berlin Heidelberg New York, pp 323–350
- McCormick CA (1999) Anatomy of the central auditory pathways of fish and amphibians. In: Popper, AN, Fay RR (eds) *Comparative hearing: fish and amphibians*. Springer, Berlin Heidelberg New York, pp 155–217
- Nieuwenhuys R, Pouwels E (1983) The brain stem of actinopterygian fishes. In: Northcutt RG, Davis RE (eds) *Fish neurobiology, vol I. Brainstem and sensory organs*. University of Michigan Press, Ann Arbor, Michigan, pp 25–64
- Palmer L, AF Mensinger (2003) Sensitivity of the anterior lateral line in free-swimming oyster toadfish, *Opsanus tau*. *Int Comp Biol* (in press)
- Popper AN, Coombs S (1982) Auditory mechanisms in teleost fishes. *Am Sci* 68:429–440
- Schellart NAM, Kamermans M, Nederstigt LJA (1987) An electrophysiological study of the topographical organization of the multisensory torus semicircularis of the rainbow trout. *Comp Biochem Physiol* 88A:461–469
- Schuijf A (1981) Models of acoustic localization. In: Tavolga WN, Popper AN, Fay RR (eds) *Hearing and sound communication in fishes*. Springer, Berlin Heidelberg New York, pp 267–310
- Sisneros JA, Bass AH (2003) Seasonal plasticity of peripheral auditory frequency sensitivity. *J Neurosci* 23:1049–1058
- Tricus TC, Highstein SM (1990) Visually mediated inhibition of lateral line primary afferent activity by the octavolateralis efferent system during predation in the free-swimming toadfish, *Opsanus tau*. *Exp Brain Res* 83:233–236
- Weeg MS, Bass AH (2000) Central lateral line pathways in a vocalizing fish. *J Comp Neurol* 418:41–64
- Wubbels RJ, Schellart NAM (1998) An analysis of the relationship between the response characteristics and topography of directional and nondirectional auditory neurons in the torus semicircularis of the rainbow trout. *J Exp Biol* 201:1947–1958
- Wubbels RJ, Schellart NAM, Goossens JHLM (1995) Mapping of sound direction in the trout lower midbrain. *Neurosci Lett* 199:179–182
- Yan H, Fine ML, Horn NS, Colon WE (2000) Variability in the role of the gasbladder in fish audition. *J Comp Physiol A* 186:435–445